

Structural Characterization of Radiation-Grafted Block Copolymer Films, Using SANS Technique

KELL MORTENSEN,¹ URS GASSER,² SELMIYE ALKAN GÜRSEL,³ GÜNTHER G. SCHERER³

¹Department of Natural Sciences, University of Copenhagen, 1871 Frederiksberg, Denmark

²Laboratory for Neutron Scattering, ETH Zurich and Paul Scherrer Institute, Villigen, Switzerland

³Research Department General Energy, Electrochemistry Laboratory, Paul Scherrer Institute, Villigen, Switzerland

Received 28 September 2007; revised 7 May 2008; accepted 8 May 2008

DOI: 10.1002/polb.21502

Published online in Wiley InterScience (www.interscience.wiley.com).

ABSTRACT: We report small-angle neutron scattering studies of grafted copolymer films of perfluorinated poly(ethylene propylene), FEP, base polymer and polystyrene, PS, grafted blocks. The films show highly anisotropic scattering patterns, revealing nematic-like ordering of the crystalline domain structure as a consequence of the processing conditions. Upon grafting, the styrene swells the amorphous domains in the copolymer formation. For styrene content beyond roughly 15%, the amorphous regimes increase on the cost of crystalline domains. To stabilize the rather well-defined domain structure already given by the original FEP base material, the samples need to be cross-linked. Without cross-linking, the nanometer length scale domains vanish, and some large scale structure takes over, likely driven by the immiscibility between FEP and PS. © 2008 Wiley Periodicals, Inc. *J Polym Sci Part B: Polym Phys* 46: 1660–1668, 2008

Keywords: fluoropolymers; graft copolymers; neutron scattering; structure; structure–property relations

INTRODUCTION

The nanoscale morphology of copolymer systems has been the subject of a large number of studies during the last years. Such nanoscale morphology has properties attractive for many types of applications. It is the nanometer-sized domain structure that makes a variety of polymers applicable for controlling rheology and wetting properties of different suspensions, ranging from motor oil to cosmetics and pharmaceuticals. The mechanical characteristics of the nanoscale domains also cause the attractive mechanical properties and processing features of thermoplastics. Different permeability and diffusion conditions within

the different domains of a nano-structured material make these materials candidates for advanced membrane systems with wide ranges of potential designable barrier properties. Such membranes have applied interests within, among others, pharmaceuticals as controlled-drug release systems, and energy materials as proton conducting membranes in fuel cells.

Different routes may be chosen to create self-associating nano-scale structured polymer materials. The given morphology may result from (i) partial crystallization where nano-meter sized crystalline domains immerse within an amorphous environment, or (ii) immiscibility between different domains (blocks) within the individual polymer molecules. For the crystallization-induced nanostructures, the detailed morphology will be determined by the characteristics of the underlying crystals.

Correspondence to: K. Mortensen (E-mail: kell@life.ku.dk)

Journal of Polymer Science: Part B: Polymer Physics, Vol. 46, 1660–1668 (2008)
© 2008 Wiley Periodicals, Inc.

In polymers composed of large segments of different monomers the degree of immiscibility between these different blocks will control the tendency to phase separate on the mesoscopic length scale, eventually resulting in ordered structures. Such ordering phenomena have been studied in great detail in the most simple polymer architecture, namely linear diblock copolymers. Their phase behavior is by now very well mapped out and understood.^{1,2} Some work has also been made on more complicated architectures like triblock and higher order linear block copolymers. The general observation is that these tend to form ordered structures on the length scale of the individual molecules when they phase separate due to intra-chain immiscibility. Simple linear diblock copolymers constitute ordered phases such as the lamellar structure, the hexagonal cylinder structure; the body centered micellar-like structure, and the complex bicontinuous gyroid structure. For higher order block copolymers even more complex structures may emerge. Another route to the formation of meso-scale domain structure in polymers relates to the tendency to form nanometer-sized crystalline domains. This is addressed in many studies, where a variety of crystallization mechanisms and domain structure are discussed. A recent study by Hsiao and coworkers review some of these studies, and present new data on the relationship between crystalline domain structure and mechanical treatment.³

While a very large number of fundamental studies exist on linear diblock copolymers, there are still only few studies revealing the phase behavior of more complex copolymer systems, like grafted and branched block copolymers. A recent study compared the morphology of respectively linear and grafted block copolymers composed of poly(vinylidenedifluoride-*co*-chlorotrifluoroethylene), P(VDF-*co*-CTFE), and sulfonated polystyrene (SPS). On the basis of TEM study, Holdcroft and coworkers showed that while the diblock copolymer form well-segregated lamellar structure, the grafted copolymer makes up an interconnected network.⁴ In the present study we discuss investigations on the mesoscale structure of a grafted diblock copolymer system based on a perfluorinated poly(tetrafluoroethylene-*co*-hexafluoropropylene), FEP, backbone, to which polystyrene, PS, chains are grafted, as illustrated in Figure 1. Such materials comprise a promising class of new nonexpensive polymer systems with tunable properties.

Journal of Polymer Science: Part B: Polymer Physics
DOI 10.1002/polb

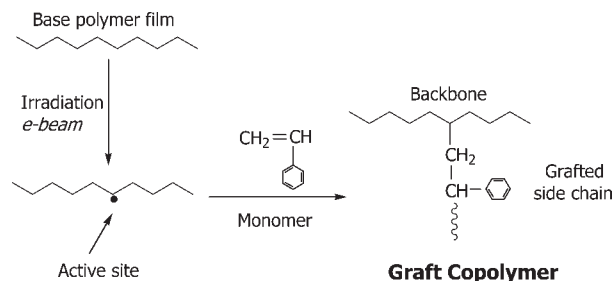


Figure 1. Schematic outline of the FEP-PS grafting procedure and structure. The cross-linker, DVB, is not shown in the scheme.

The material has particular interests for potential application as membrane material in polymer fuel cells and is studied intensely in this context. Proton conductivity may be introduced into these copolymers by sulfonating the polystyrene segments. In addition, cross-linking the polymer system has been found to have a positive effect on the polarization as well as on the durability. The ohmic resistance, on the other hand, generally increases as a function of cross-linker content.⁵

Membranes based on per-fluoro sulfonic acid polymers (PFSA) (e.g., Nafion[®] DuPont) have served as standard and reference fuel cell materials for several decades⁶ and are now commercially utilized as solid electrolyte on a worldwide scale in chlor alkali cells. Some studies have been reported elucidating the phase separated morphology of Nafion and other membrane materials on a nanoscopic scale and relate them to properties like swelling, ionic conductivity, permeability, mechanical properties, and so forth, which are of utmost importance for their use in for example, electrochemical cells.^{7–13}

The understanding of structure–property relationships is important for the studied radiation-grafted membranes. In particular because there are several constraints related to the selection of materials and processes involved. We present in this article small-angle neutron scattering results on pristine FEP films as well as on crosslinked and uncrosslinked FEP-*g*-PS grafted copolymer films that are not sulfonated. We find that already the pristine FEP material is dominated by a nanoscale domain structure as imposed by the partial crystalline base material. While the grafting clearly causes swelling and likely changing of the crystalline/amorphous ratio, we see no additional nanoscale organization as induced by the FEP-PS immiscibility.

The processed FEP-polymer film shows marked anisotropy, as a result of the extrusion process applied during production. Typically, properties measured in machining direction are accordingly different from the ones in perpendicular direction. This structural anisotropy remains both during the grafting process and during the successive sulfonation and crosslinking. The grafting process has previously been shown to follow a grafting front mechanism,¹⁴ whereby the monomers to be grafted have to intrude to the middle of the film starting from the film surface, hence also building-up local concentration gradients of the grafted components, which also cause a locally different ionic concentration.

EXPERIMENTAL

Structural studies using small-angle neutron scattering technique (SANS) were carried out on FEP base polymer films grafted with PS to varying degree within the range of 0–50% mass concentration. SANS was used for structural investigations primarily because of the forthcoming extended contrast variation studies in membranes swollen with water.¹⁵

Material

The copolymer synthesis is sketched in Figure 1. The graft copolymerization reaction was performed via radiation-induced grafting method using FEP as the base film and styrene as the monomer. Styrene is an ideal monomer for grafting, since the aromatic ring is easily sulfonated to introduce ion exchange functionality for proton conducting membrane applications. No sulfonation was performed for this study. Divinyl benzene (DVB) was introduced to the grafting solution for the preparation of cross-linked grafted films.

The base polymer, FEP, (purchased from DuPont, Circleville, OH) was made into 25- μ m-thick films, which were activated using an electron beam (Studer AG, Däniken, Switzerland) with a total dose of about 3–6 kGy. The films were successively stored at –80 °C until grafting was initiated.

For the grafting, the irradiated films were introduced into a stainless steel reactor containing the grafting solution. In the uncrosslinked systems, the grafting solution consisted of 120-mL styrene (Fluka purum) in 330 mL isopropanol

and 150 mL deionized water. The solutions were purged with nitrogen for 1 h, and then the reactor was placed in a water bath at 60 °C for 20 min up to 24 h. The films were removed from the reactor, washed with toluene to remove polystyrene homopolymer, and finally dried under vacuum at 80 °C until the films reached a constant weight. The degree of grafting (DG) based on mass percent was defined according to

$$DG = \frac{W_g - W_0}{W_0} \quad (1)$$

where W_0 and W_g are the weights of the film before and after grafting, respectively. Grafting is found to occur initially at the surface of the film, then proceeds gradually inwards as the grafting zone is swollen by the monomer.¹⁶

For crosslinking the copolymer system, we used DVB purchased from Fluka (technical grade). The crosslinked systems were made using a procedure similar to that described above, but with the grafting solution consisting of a 120 mL mixture of styrene and DVB dissolved in 330 mL isopropanol and 150 mL deionized water. The ratio of DVB and styrene was varied in the range from 0:1 to 1:4 (v/v). The degree of crosslinking C_{x-link} is defined according to:

$$C_{x-link} = \frac{V_{DVB}}{V_{PS} + V_{DVB}} \quad (2)$$

where V_i is the volume of respectively, PS or DVB. Radiation grafted membranes cross-linked with DVB were found to have lower surface energy and hydrophilic character, which will influence the membrane electrode interface if used in fuel cell applications. The water uptake reported was significantly reduced and concomitant lower proton conductivity was measured.¹⁷

Samples prepared for the SANS experiments were folded to make films of roughly 0.8 mm thickness, keeping the processing direction parallel to the vertical axis of the scattering plane.

SANS Experiments

SANS experiments were performed using the SANS-II instrument at the Paul Scherrer Institute, PSI, in Switzerland, and the NG3 SANS facility at NIST in USA. The latter instrument was used for the spectra obtained on systematic

varying degree of crosslinking, as shown in Figure 8 below.

The PSI-SANS experiments were done with a neutron wavelength equal to 5.6 Å and sample-to-detector distance equal to 1.2 and 3 m; and with 12 Å neutrons with sample-to-detector distance equal to 6 m. The NIST-SANS experiments were performed using 6 Å neutrons with sample-to-detector distances 1.3 and 7 m as well as 8.4 Å neutrons with a sample-to-detector distance of 13.2 m. The NIST SANS data at 13.2 m were obtained using the module of compound-refractive lenses focusing the beam at the detector. This allowed for structural characterization to q -values down to 0.001 Å^{-1} , where q is momentum transfer: $q = 4\pi/\lambda \sin \theta$ given by the scattering angle 2θ and the neutron wavelength λ .

The SANS data were calibrated for detector nonlinearity using the incoherent scattering from 1-mm-thick water, according to standard procedures. In the following we show both two-dimensional presentation of $I(\mathbf{q})$ -data, and one-dimensional $I(q)$ data calculated in a section of $\pm 0.0013 \text{ Å}^{-1}$ around the vertical axis (see Fig. 2).

RESULTS AND DISCUSSION

Figure 2 shows the two dimensional scattering patterns as obtained from pristine films of FEP and grafted copolymers of FEP base with different amounts of polystyrene, PS. The figures show both films that have been cross-linked with divinylbenzene, DVB (right column), and films without cross-links (left column).

Anisotropy

All scattering patterns show pronounced anisotropy in the range $q < 0.04 \text{ Å}^{-1}$, with high intensity in the machining direction of the processed film, while the scattering intensity perpendicular is markedly reduced. This finding is to some extent analogous to what is observed in Nafion films, which show indication of anisotropic alignment similar to our observations with respect to the domain structure originating from crystalline domains in the polymer matrix, while the anisotropy of the ionomer clusters have the more common alignment parallel to the machining direction.^{18,19} The scattering pattern of both the pristine FEP film and the cross-linked samples are dominated by a correlation peak in the

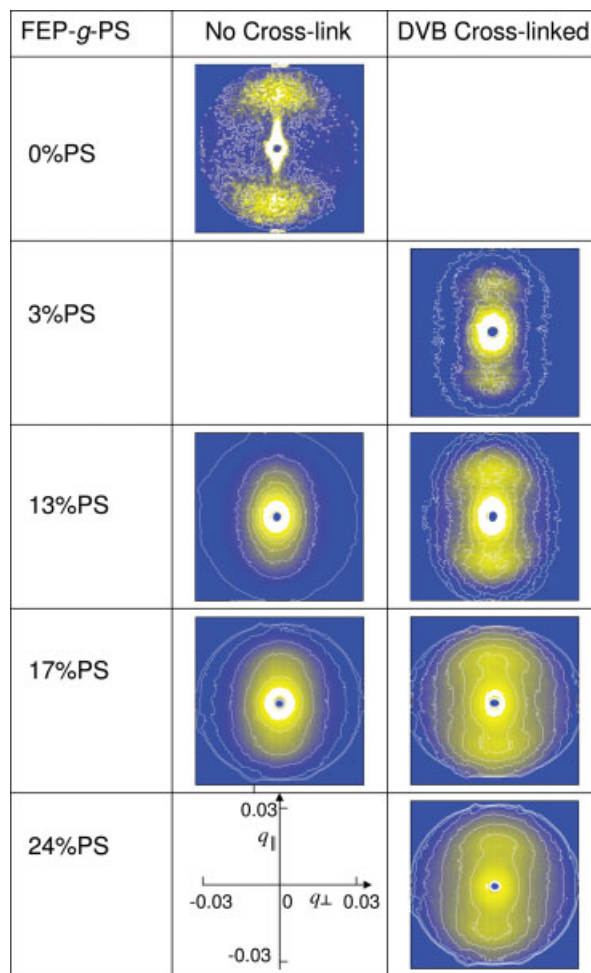


Figure 2. Two dimensional scattering patterns of FEP-PS grafted copolymers with different grafting density. The left row shows data of polymers with no cross-link, while the column at right shows samples cross-linked with DVB. The machining direction is vertical in the plots.

range $0.015\text{--}0.02 \text{ Å}^{-1}$, while the scattering intensity of the non-cross-linked grafted samples tends to decrease monotonically with scattering momentum within the q -range measured.

The anisotropy in these samples seems limited to a q -range $0.005\text{--}0.05 \text{ Å}^{-1}$, corresponding to length scales of the order of $120\text{--}1200 \text{ Å}$. This is seen from the two-dimensional plots given in Figure 2, and more clearly in Figure 3 showing the two scattering functions as calculated from the two-dimensional data along the vertical axis (parallel to machine direction) and the horizontal axis (perpendicular to machine direction), respectively. At large q -values the two scattering functions approach the Porod law, $I(q) \sim q^{-4}$ of an isotropic system of solid smooth interfaces.

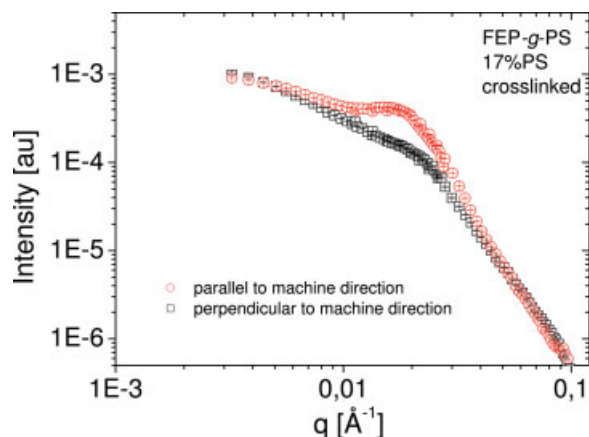


Figure 3. Anisotropic scattering functions as exemplified by the sector averaged $I_{\parallel}(q)$ and $I_{\perp}(q)$ data for cross-linked FEP-PS grafted copolymers with degree of grafting: DG = 17%. [Color figure can be viewed in the online issue, which is available at www.interscience.wiley.com.]

Both these high- q characteristics and the low- q isotropic properties need more investigations. The marked anisotropy may in a first attempt be explained in a simple picture as that shown in Figure 4(a). FEP is known to be partial crystalline, having crystalline domains embedded in an amorphous FEP matrix.²⁰ The scattering anisotropy is likely a consequence of the machining, where anisotropic crystalline domains orient perpendicular to the machining direction in a nematic-like manner. The degree of anisotropy may formally be evaluated using the order-parameter, P_2 .²¹

$$P_2 = 1 - \frac{3}{2\Phi} \int_0^{\pi/2} I(\phi + \pi/2) \times \left[\sin^2 \phi + \sin \phi \cos^2 \phi \ln \left(\frac{1 + \sin \phi}{\cos \phi} \right) \right] d\phi \quad (3)$$

derived to characterize the orientational order of nematic-like objects with a distinguished axis, $I(\phi)$ being the intensity depending on the azimuthal angle ϕ , and Φ being a normalization constant

$$\Phi = \int_0^{\pi/2} I(\phi + \pi/2) d\phi.$$

With P_2 calculated within the q -range 0.01–0.02 Å^{−1} characteristic of the peak-position, we

find a P_2 -value of the order of 0.2, highest for the pristine FEP material ($P_2 = 0.26$) and lowest for the grafted uncrosslinked FEP-PS copolymers ($P_2 \approx 0.16$). The anisotropy is reflected by the mechanical properties of the films. The base FEP film has a tensile strength of 36.3 MPa along the machining direction and 27.6 MPa transverse to this. The corresponding values of the Young's modulus are 488.8 MPa (480.7 MPa), respectively. The correlation between the degree of anisotropy and the mechanical properties with processing conditions will be the focus of a forthcoming study.

Structural Dependence on Grafting Density

Figure 5 shows the scattering function $I(q)$ of the pristine FEP polymer film, and films of grafted and cross-linked FEP-g-PS, as calculated from the data shown in Figure 2, averaging within a section of ± 0.0013 Å^{−1} around the vertical axis. Two features clearly appear from these data. First of all the scattering intensity grows dramatically upon grafting, second the peak position changes systematically to lower values upon grafting.

From thermogravimetric analysis (TGA) as well as scanning differential calorimetry (DSC) studies^{20,22,23} it is known that the styrene-monomers predominantly graft the amorphous FEP regimes, causing swelling of this phase as seen in the decreasing peak position, q^* . The marked increase in intensity reflects the very large contrast between PS and (crystalline-) FEP in relation to the much lower contrast between

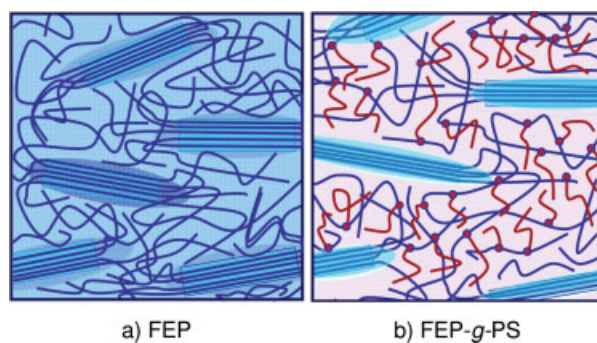


Figure 4. Schematic illustration of the amorphous-crystalline domain structure in pristine FEP polymers (a) and cross-linked PS-grafted films where PS predominantly goes into the amorphous regimes (b). [Color figure can be viewed in the online issue, which is available at www.interscience.wiley.com.]

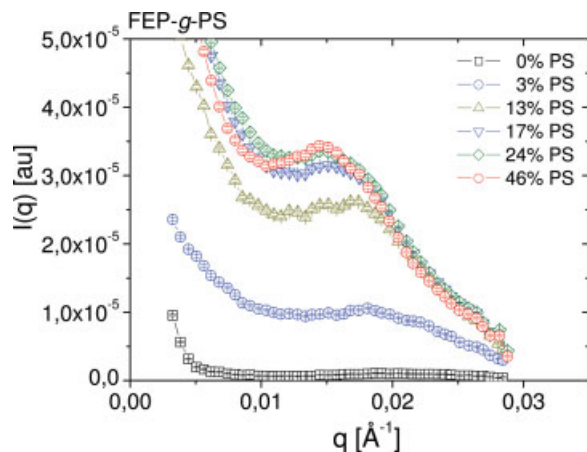


Figure 5. Sector averaged $I_{\parallel}(q)$ data for cross-linked FEP-PS grafted copolymers for different degree of grafting: DG = 0, 3, 13, 17, 24, and 46%. [Color figure can be viewed in the online issue, which is available at www.interscience.wiley.com.]

amorphous and crystalline FEP being the origin of scattering from the pristine FEP material. This situation is sketched in Figure 4(b), where the red chains (light grey) represent PS-blocks and the blue (dark grey) represent FEP-chains.

The systematic change in q^* of the correlated structure and the intensities at the peak-value, $I(q^*)$, are shown in Figure 6. In the figure we give the real space correlation length, d , defined as

$$d = \frac{2\pi}{q^*} \quad (4)$$

rather than q^* itself. We point out that d is strictly not the simple average distance between, for example, crystalline domains. d is a distance characteristic for the system, determined by a complex combination of inter-domain distances, domain form, and the effective interaction between adjacent domains.

The results given in Figure 6 show regular increase in both characteristic distance, d , and intensity $I(q^*)$ with grafting density in the range 0–15%, while both intensity and distance (or q^*) remain basically constant for PS content more than 15%. One may argue that the characteristic distance of crystalline domains increases slightly more abrupt from 0 to 3% PS content, however, the broad correlation peaks as seen in Figure 5 do not really give a very well defined value. Grafting beyond 3% causes a continuous increase in characteristic length until roughly DG = 10–15%, beyond which value the distance

remains roughly constant. The intensity is more well-defined, and shows a roughly linear increase with PS content until a plateau is reached around 15% grafting density.

These observations should be correlated to former observations that grafting occurs initially at the surface of the film, and then proceeds gradually inwards as the grafting zone is swollen by the monomer.^{14,16} Only for grafting densities beyond roughly 10%, that is, close to the cross-over value observed by SANS, seems the film to be uniform with respect to PS concentration. The SANS data support these observations. The scattering data indicate though that the process is not just a simple “moving” front of grafted PS. If this was the case, we should have observed the rather abrupt change in q^* from the 0 to the 3% grafting level, and a constant value beyond this, since the scattering function due to contrasts is totally dominated by the part of the sample where both PS and FEP are present. The continuous increase in $d = 2\pi/q^*$ within the 3–15% range reveals that the PS density still increases inside the domain structure also in this range.

For grafting densities beyond roughly DG \approx 15% no further changes appear. This may indicate

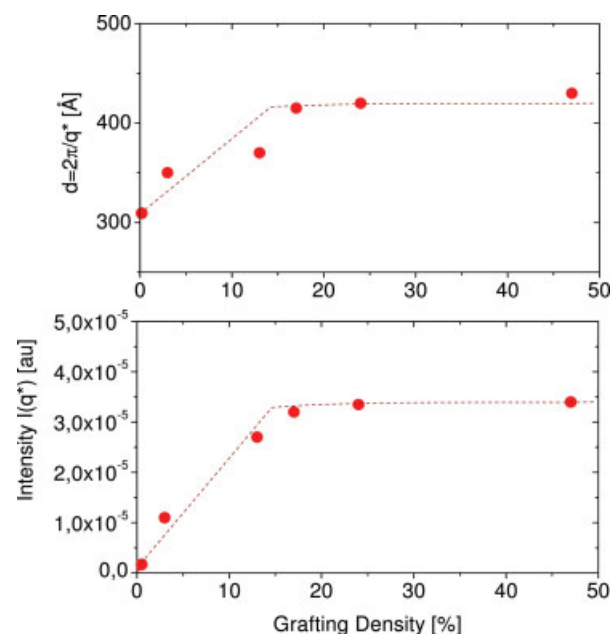


Figure 6. Characteristic length-scale $d = 2\pi/q^*$ and the peak-intensity $I(q^*)$ as obtained from the data shown in Figure 5. [Color figure can be viewed in the online issue, which is available at www.interscience.wiley.com.]

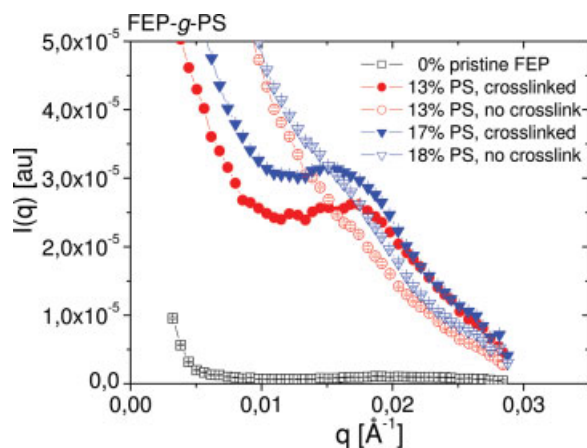


Figure 7. Sector averaged $I_{||}(q)$ data for cross-linked and non-cross-linked FEP-PS grafted copolymers for different degree of grafting: DG = 0, ~13 and ~17%. [Color figure can be viewed in the online issue, which is available at www.interscience.wiley.com.]

that the amorphous FEP-*g*-PS domains increase in size on the cost of crystalline FEP. Both the characteristic distance between crystalline domains, and the contrast between these domains remain unchanged, giving the rather constant scattering function. In reality, of course, the peak position is not only given by the interdomain spacing and contrasts, but also the shape and mutual correlations. But the experiments show that to first approximation it seems correct to use such a simple model.

Structural Dependence on Crosslinking

We notice in the two-dimensional scattering patterns displayed in Figure 2 and the corresponding one-dimensional intensity, $I_{||}(q)$, shown in Figure 7 that only the scattering patterns of cross-linked polymers show the regular changes in correlation peak with grafting density. Without cross-linking, the correlation peak apparently vanishes, or at least is hardly visible as due to very high scattering intensities due to some larger scale fluctuations. For comparison, we have also included the pristine FEP data in Figure 7.

The major difference between cross-linked and uncrosslinked samples is clearly a significant increase in low- q scattering of the uncrosslinked samples, and a significant reduction in the correlation peak, if apparent at all in the

uncrosslinked samples. As known from TGA and DSC measurements,^{20,22,23} the PS and FEP polymers are most likely nonmiscible. One should therefore expect microphase separation of the PS and FEP units causing the formation of domains rich in PS embedded in a FEP-rich matrix. Such immiscibility driven mesoscopic domain structures are not visible within the measured q -range shown in Figures 2 and 7, but it is possible that the significant small-angle scattering in the non-cross-linked samples reflects such properties. The immiscibility between PS and FEP may cause some kind of domain structure that apparently reaches far beyond the length-scale of the individual copolymer units.

To further investigate this, we made extended scattering experiments using the compound lens system at the NIST instrument to measure at even lower scattering momentum. Figure 8 shows the resulting azimuthally averaged $I(q)$ -function for FEP-*g*-PS copolymers with DG = 19% and varying cross-link densities in the range 0–20%. These low- q data clearly indicate the formation of large scale structural density fluctuations, with a correlation peak, $q^* \approx 0.0035 \text{ \AA}^{-1}$ corresponding to length scales of the order of 1800 Å, that is, far beyond the length scale of expected polymer blocks of the system. The low- q peak is most pronounced in samples without crosslinks (0% DVB), and vanishes strongly with crosslinking. While it seems quite

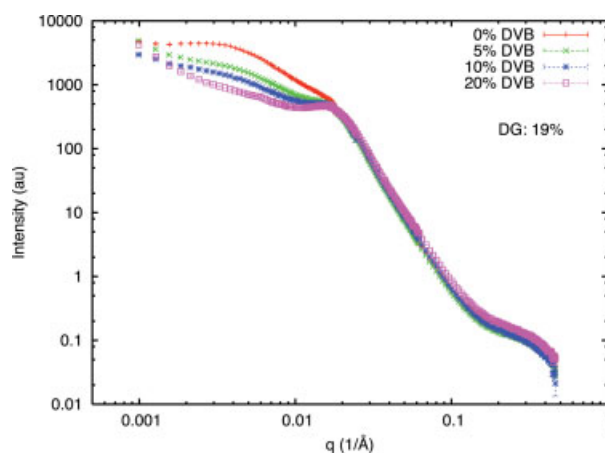


Figure 8. Azimuthally averaged $I(q)$ data for FEP-*g*-PS copolymer films cross-linked to different degree: $C_{x-link} = 0, 5, 10$, and 20%. The grafting density was 19% for all samples. [Color figure can be viewed in the online issue, which is available at www.interscience.wiley.com.]

likely that the large scale domain structures are formed due to immiscibility of PS and FEP, the underlying structure still remains to be solved. That very long PS-chains can be obtained by grafting in a nonsolvent has also been observed in the PS-grafting of polyethylene films.²⁴

In the cross-linked copolymers, the polymer blocks are mutually fixed by the cross-linking sites, and thermal equilibration in the form of large scale structures is prohibited. The cross-linked samples are therefore needed to overcome effects of immiscibility and make films and membranes where the domain structure is given by the length scale of the original crystalline/amorphous properties.

CONCLUSIONS

The present SANS studies have shown regular dependence on grafting density and cross-linking. The structural properties of the base FEP films are highly modified by the processing conditions, as revealed by a substantial anisotropy in the structural properties, indicating crystalline domains oriented perpendicular to the machining direction.

Upon grafting FEP base-polymers with styrene monomers, the styrene swells the amorphous domains in the copolymer formation. In cross-linked films with polystyrene content beyond roughly 15%, the amorphous regimes seem to increase on the cost of crystalline domains. To stabilize the rather well defined domain structure already given by the original FEP base material, the samples need to be cross-linked. Without cross-linking, the nanometer length scale domains vanish, and some large scale structure takes over. It may be speculated that these large scale structures somehow are driven by the immiscibility between FEP and PS.

To some surprise, our study fails to show correlated structure on the length scale of individual polymer block size, as induced by the PS-FEP immiscibility. Such correlated structures are the dominant feature seen in both linear block copolymers, like diblock and triblock copolymers,^{1,2} and in more complex systems like for example interpenetrating copolymer networks.²⁵ In the non-cross-linked FEP-g-PS, on the other hand, ≥ 200 -nm large domain structures appear, likely related to the immiscibility.

The underlying structural origin determining the size and other characteristics of these large scale domains is still unresolved, however.

The large scale domain structure formation is completely prevented by cross-linking the polymer system. In that case the dominating structure is still governed by the original alternating crystalline/amorphous structure given by the FEP base polymer.

This work was supported by the Danish Instrument Center for Neutron Scattering (DANSSK) sponsored by the Danish Research Council for Nature and Universe. The majority of the experimental work was performed at the Swiss spallation neutron source SINQ, Paul Scherrer Institute, Villigen, Switzerland. We further acknowledge the support of the National Institute of Standards and Technology, U.S. Department of Commerce, in providing the neutron research facilities used in this work, and illuminating discussions with Boualem Hammouda. The NIST work utilized facilities supported in part by the National Science Foundation under Agreement No. DMR-0454672.

REFERENCES

1. Bates, F. S.; Schultz, M. F.; Khandpur, A. K.; Förster, S.; Rosedale, J. H.; Almdal, K.; Mortensen, K. *Trans Faraday Soc* 1994, 98, 7–18.
2. Hamley, I. *The Physics of Block Copolymers*; Oxford Science: USA, 1999.
3. Kawakami, D.; Burger, C.; Ran, S.; Avila-Orta, C.; Sics, I.; Chu, B.; Chiao, S.-M.; Hsiao, B. S.; Kikutani, T. *Macromolecules* 2008, 41, 2859–2867.
4. Tsang, E. M. W.; Zhang, Z.; Shi, Z.; Soboleva, T.; Holdcroft, S. *J Am Chem Soc* 2007, 129, 15106–15107.
5. Gubler, L.; Gürsel, S. A.; Scherer, G. G. *Fuel Cells* 2005, 5, 317–335.
6. Doyle, M.; Rajendran, G. In *Handbook of Fuel Cells: Fundamentals, Technology, Applications*; Vielstich, W.; Lamm, A.; Gasteiger, H. A., Eds.; Wiley: New York, 2003; Chapter 30, Vol. 3, pp 349–351.
7. Register, R. A.; Cooper, S. L. *Macromolecules* 1990, 25, 318–323.
8. Kreuer, K. D. *J Membr Sci* 2001, 185, 29–39.
9. van der Heijden, P.; Rubatat, L.; Diat, O. *Macromolecules* 2004, 37, 5327–5336.
10. Kim, M.-H.; Glinka, C. J.; Grot, S. A.; Grot, W. G. *Macromolecules* 2006, 39, 4775–4787.
11. Young, S. K.; Trevino, S. F.; Tan, N. C. B. *J Polym Sci Part B: Polym Phys* 2002, 40, 387–400.
12. Rubatat, L.; Shi, Z.; Diat, O.; Holdcroft, S.; Frisken, B. J. *Macromolecules* 2006, 39, 720–730.
13. Gao, J.; Lee, D.; Yang, Y.; Holdcroft, S.; Frisken, B. J. *Macromolecules* 2006, 39, 8060–8066.

14. Gupta, B.; Scherer, G. G. *Chimia* 1994, 48, 127–137.
15. Gasser, U.; Mortensen, K.; Alkan-Gürsel, S.; Scherer, G. G., unpublished work.
16. Chapiro, A. *Radiation Chemistry of Polymeric Systems*; Wiley: New York, 1962.
17. Büchi, F. N.; Gupta, B.; Haas, O.; Scherer, G. G. *Electrochim Acta* 1995, 40, 345–353.
18. Blanchot, J. F.; Diat, O.; Putaux, J.-L.; Rollet, A.-L.; Rubatat, L.; Vallois, C.; Muller, M.; Gebel, G. *J Membr Sci* 2003, 214, 31–42.
19. Mauritz, K. A.; Moore, R. B. *Chem Rev* 2004, 104, 4535–4585.
20. Gupta, B.; Scherer, G. G. *Die Angew Makromol Chem* 1993, 210, 151–164.
21. Deutsch, M. *Phys Rev A* 1991, 44, 8264–8270.
22. Gupta, B.; Highfield, J. G.; Scherer, G. G. *J Appl Polym Sci* 1994, 51, 1659–1666.
23. Gupta, B.; Haas, O.; Scherer, G. G. *J Appl Polym Sci* 1994, 54, 469–476.
24. Berg, R. H.; Almdal, K.; Pedersen, W. B.; Holm, A.; Tam, J. P.; Merrifield, R. B. *J Am Chem Soc* 1989, 111, 8024–8026.
25. Ivan, B.; Almdal, K.; Mortensen, K.; Johannsen, I.; Kops, J. *Macromolecules* 2001, 34, 1579–1585.